Effect of Iron on the Hot Cracking of Uranium Weld Metal—Part I

Iron is added in calculated amounts to electron-beam welds, and hot cracking susceptibility is determined with a spot-Varestraint test device

BY P. W. TURNER AND C. D. LUNDIN

ABSTRACT. The influence of iron on the hot-cracking tendency of uranium weld metal was investigated. Iron was added in calculated amounts to electron-beam welds to produce weld-metal compositions ranging from 50 to 7,700 ppm iron. Hot cracking susceptibility was determined with a spot-Varestraint test device. Intermediate iron concentrations in the weld metal caused severe cracking at low levels of strain. Welds having high and low concentrations of iron were not prone to hot cracking. The cracking tendencies of actual welds on partial penetration butt joints compared favorably with the results of the Varestraint test.

Introduction

The maximum impurity level of iron that can be tolerated in uranium without causing fabrication problems has not been well defined. Excessive amounts of the usual impurities are known to cause cracking in hot working and welding operations. A much used "rule of thumb" suggests that the total impurity content should not exceed 1,000 ppm. The approach has been to produce relatively high-purity uranium rather than to specify upper limits for the concentrations of impurities that may lead to fabrication or service problems. This cautious attitude exists because quantitative information relating the effect of impurity elements to metal processing behavior is lacking.

When fabrication difficulties occur, the question of impurity level requires attention. One area of concern is the fusion welding of wrought and cast uranium. The base metal usually contains fractions of recycled scrap that accrue from metal fabricating steps. Since one of the most common contaminants in recycled scrap is iron, the effect on the properties of uranium weld metal is of practical interest.

Features of the uranium-iron constitutional diagram suggest that welds of low iron compositions may be susceptible to cracking as the weld metal cools through the liquidus-solidus temperature interval. A uranium-iron phase diagram,[1–4] showing the range of interest, is presented in Fig. 1. The low solid solubility and the wide freezing range at low iron levels are normally characteristic of alloys that are hot short.

The detrimental effect of the wide freezing range may be aggravated further by the nonequilibrium conditions existing during freezing of weld metal. The effective solidus is depressed by coring and lack of time for diffusion. Likewise, peritectically reactive liquid may tend to persist and solidify at temperatures descending to the eutectic reaction isotherm.

The foregoing considerations led to this investigation[5] to determine the influence of iron on the hot-cracking tendency of uranium weld metal.

Objectives and Scope

The primary purpose of this work was to determine the effects produced by small alloying additions of iron on the hot-cracking tendency of uranium weld metal. In this presentation, the term "hot cracking" relates to cracking that occurs during weld-metal solidification by what is generally believed to be a liquation mechanism. Analogous terms are "hot tearing" and "fissuring."

The scope of the experimental program included:

1. The design and fabrication of a modified Varestraint test device.
2. Development of a procedure for doping welds in high-purity uranium with iron.
3. Testing welds for their hot-cracking tendency at various levels of iron, and the correlation of results with iron concentration.
4. Identification of constituents responsible for hot cracking.
5. Establishment of a model for cracking.
6. Comparing the incidence of cracking in an actual welded joint with the results of the hot-cracking test.

This paper is Part I of a two-part study; it deals with laboratory hot-cracking tests and the correlation of results with practice. In Part II, which shall be prepared later, the cause of cracking is more clearly defined and a model describing the cracking is developed from metallurgical analyses, hot-cracking test data, and tests on welded joints.

Materials

Base metal was comprised of wrought uranium plates prepared from a single heat. Chemical analyses for the major impurities in the unalloyed base metal are presented in Table 1. Photomicrographs in Fig. 2 show the annealed alpha structure. Grains are equiaxed with some twinning. A few inclusions are visible in the bright field view. High-purity iron wire and foil were used to dope the weld bead. Chemical analyses are presented in Table 2.

Experimental Procedures

Doping Procedure

The diagram in Fig. 3 shows the method of preparing the uranium plates which were doped with iron for this study. An electron-beam weld was made along the groove after filler

P. W. TURNER is Supervisor, Welding Development Laboratory, Oak Ridge Y-12 Plant, Union Carbide Corp., Nuclear Division, Oak Ridge, Tenn.; C. D. LUNDIN is Associate Professor, Chemical and Metallurgical Engineering Dept., The University of Tennessee, Knoxville, Tenn.

Paper presented at the AWS 51st Annual Meeting held in Cleveland, Ohio during June 8-12, 1970.

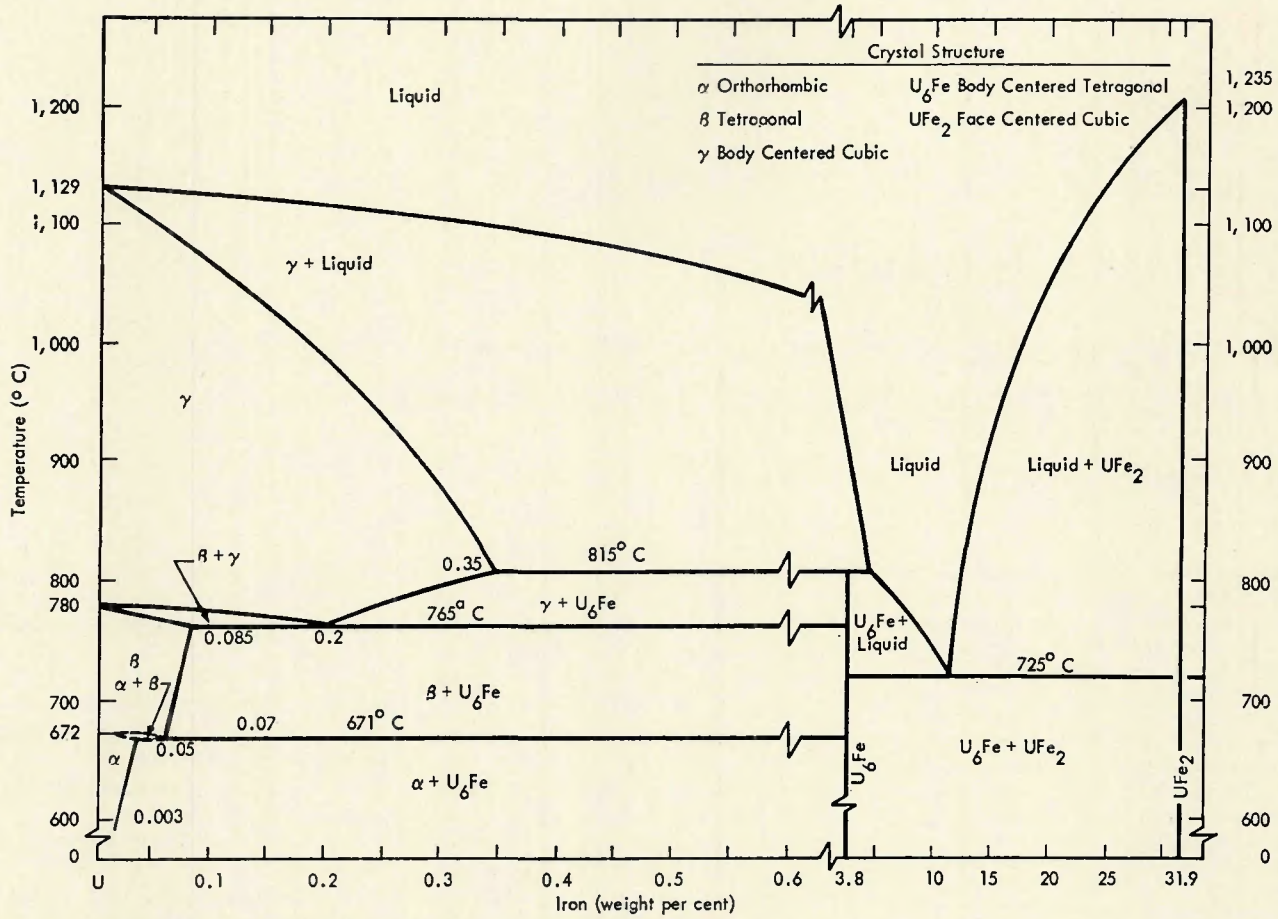

Fig. 1—Uranium-rich section of the uranium-iron phase diagram

metal strips and iron doping material were placed in the groove. The strips and the measured amount of iron were fused into the base metal to form an alloyed weld bead (Fig. 4) by the electron-beam weld pass. The iron placed in the weld groove was held in position by the uranium filler metal strips. Foil, wire, and iron vapor deposited onto uranium strips were the specific configurations used to provide iron for doping the weld. The wire was used as a source material in the procedure which vapor deposited small amounts of iron onto the strips; also, the wire itself was used as an insert in the groove to obtain higher iron contents. Chemical analyses of both the wire and the foil are listed in Table 2.

The uranium strip filled several functions; these were to:

1. Provide the weld with a buildup which was milled for chemical analysis.
2. Hold the preplaced iron alloying addition in place during welding.
3. Shield the iron from direct impingement of the heat source to prevent excessive vaporization and premature melting.
4. Provide a simple substrate on which iron could be vapor deposited.

The iron contents of hot-cracking test specimens taken from these plates ranged from the base-metal composition (50 ppm) up to 7,700 ppm.

Chips, milled from the weld reinforcement of each specimen, were analyzed for iron by atomic absorption analysis. Uranium analyses were accomplished by an X-ray absorption procedure. The repeatability of analyses for iron is indicated in Table 3.

This alloying technique is different from the more usual practice of making individual heats having different concentrations of the alloying element of interest. Because only a single melt was utilized, the effects of the primary processing variables and of trace elements were invariant in the experiment.

Table 1—Major Impurities in Uranium Base Metal

Element	Concentration, ppm[a]
Aluminum	< 10
Carbon	54
Copper	5
Hydrogen	2 ppm (by volume)
Iron	50
Lead	5
Magnesium	15
Manganese	15
Nickel	15
Nitrogen	14 ppm (by volume)
Oxygen	30 ppm (by volume)
Phosphorus	<100
Silicon	60
Tungsten	<100

[a] Parts per million by weight unless otherwise indicated.

Modified Varestraint Test

Recently, a second-generation Varestraint test was developed at the Rensselaer Polytechnic Institute. It has been referred to as a "Spot-Varestraint test," a "modified-Varestraint test," and, colloquially, as a "Tigamajig." The inability of the original Varestraint method to accommodate a subscale specimen stimulated the design of this test device. Goodwin has described the features of this test and used it in studying hot cracking in Inconel 600.[6] A similar device, shown schematically in Fig. 5, was built and utilized in the present study.

The modified Varestraint test requires an arc-spot weld at the midspan of a specimen which is fixed at each end. The face of the spot is bent in tension while the fusion zone of the spot is still molten. This test evaluates the hot-cracking tendency of a specimen prepared either from base material or from previously deposited weld metal. The specimen is subjected to an arc-spot welding thermal cycle,

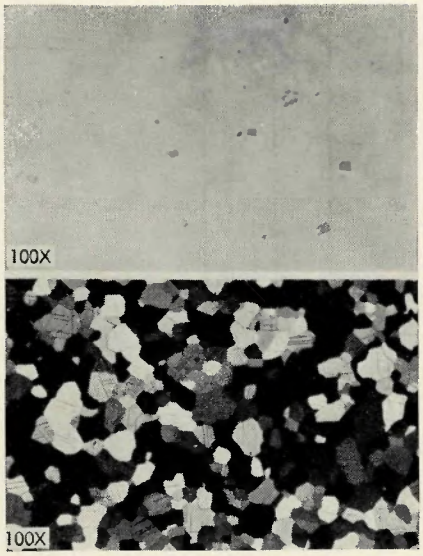

Fig. 2—Structure of wrought and annealed uranium base metal (reduced 60% on reproduction)

and the hot zone is strained a predetermined amount while the spot fusion zone is still molten. The material surrounding the spot is subjected to the thermal distribution produced by the welding operation, and the metallurgical structure is altered in much the same manner as in a standard arc weld. Thus, this test permits the metallurgical factors to be controlled while the augmented strain of successive specimens is varied in incremental amounts. This feature makes possible a quantitative assessment of the susceptibility for hot cracking. The augmented strain in the outer fibers of the specimen is expressed as follows:

Tangential augmented strain $= \epsilon \cong \frac{t}{2R}$, in which R, the bending radius, is much greater than t, the thickness of the specimen.

An important difference between this test and the conventional Varestraint test relates to the thermal history of the weld bead. In the conventional test, the augmented strain is applied as the weld test bead is being made. In the modified test, strain is applied while an existing weld bead is being remelted locally by an arc-spot welding process. This ability to test welds that have been made at some prior time makes the modified test a flexible analytical tool. It is ideally suited for checking the effect of multipass weld beads on previously deposited weld metal and for evaluating the cracking propensity of overlapping or intersecting weld beads. Its use is, of course, not limited to these special cases.

The specimen for the modified test can be much smaller than the one for the conventional test. This feature is a very dominant one when the supply of material is scarce or when an investigation involves either costly material or a large number of specimens.

A pictorial view of the spot-Varestraint test device used in this program is shown in Fig. 6 with the test specimen and gas-cooled torch in position.

Table 2—Analyses of Iron Alloying Additions

Element	Foil[a]	Wire[a]
Carbon	180	—
Manganese	177	500
Phosphorus	70	100
Silicon	30	50
Sulfur	231	100
Iron	99.48 wt-%	99.97 wt-%
Insoluble in H_2SO_4	—	300

[a] Parts per million unless otherwise noted.

Tigamajig Testing Procedure

A general layout of the testing area is illustrated in Fig. 7. The air cylinder and piping assembly are below the table on which the enclosed superstructure of the test device is mounted. The welding power supply is beside the table. Ancillary equipment consists of a Wollensak Fostex, high-speed, 16 millimeter, WF3 camera and a Model 320 Sanborn, two-channel recorder.

The testing procedure involves the technique of fixing the specimen in the test device and the application of force to bend it during spot welding.

Force was not measured directly; instead, air pressure on the four-inch-diameter cylinder was regulated at 80

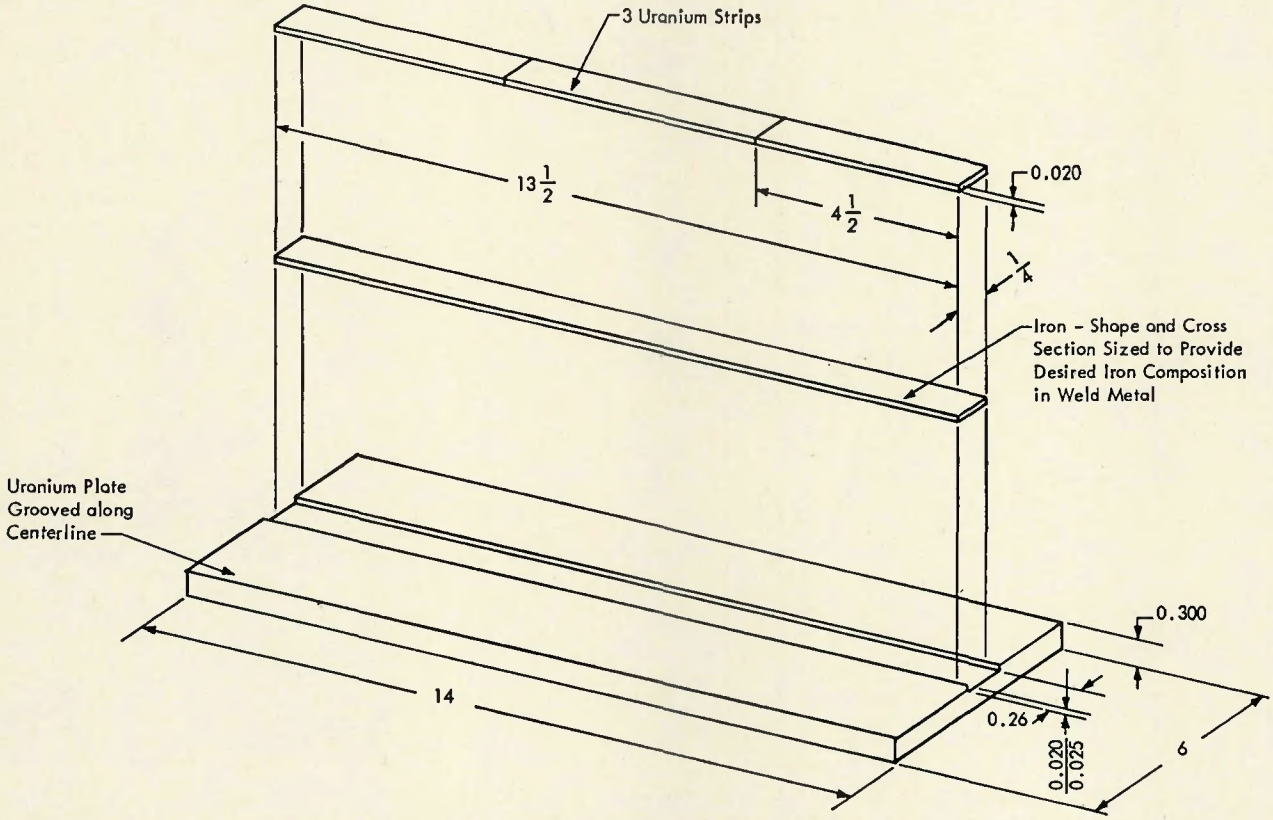

Fig. 3—Geometry and components of the plate assemblies for weld-metal studies

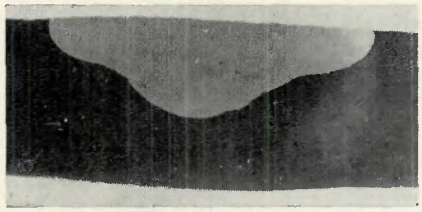

Fig. 4—Profile of an electron-beam weld doped with 4,900 ppm iron. (Electrolytic etch in 50 volume-% phosphoric acid solution)

Table 3—Repeated Analyses of Iron in Uranium Weld Metal

Specimen	Plate	Plate position	Iron, ppm 1. Milled	2. Drilled	3. Drilled
52	2	1	1,200	1,384	1,406
55	4	12	1,433	1,402	—
62	2	2	1,520	1,366	—
64	3	2	667	642	—
65	3	1	704	934	—
109	9	12	216	460	—
129	4	6	967	1,000	—

psig. The period between the time the arc was extinguished and the time the bending force caused the specimen to move was 45 milliseconds. The spot weld appeared to be solidified 0.2 sec after the arc was terminated. Thus, straining was accomplished while the spot weld was still in the molten state.

Specimens were adjusted in the grips of the test device by tapping the wedge (Figs. 5 and 6) lightly with a small hammer while the nuts holding the grips were finger tight. This step removed the slack between the dowel pins of the grips and holes in the specimen. Then the grips were tightened by applying a 25 ft-lb torque to the hold-down nuts. The welding and straining portions of the test were then conducted.

After the arc was extinguished, a flow of helium at 60 cfh was applied for 90 sec to shield the specimen as it cooled. Then the specimen was removed from the grips. The temperature at this stage was approximately 135° F at the edge of the specimen adjacent to the spot. The peak temperature during the welding cycle was 970°F at this location.

Hot-Cracking Test Results

General Observations

During the initial testing of unalloyed (pure) uranium, several characteristic surface features of the as-welded and strained specimens were noted. The macrograph shown in Fig. 8 illustrates the typical appearance of the surface of a strained pure uranium sample. Immediately below this macrograph is a schematic representation of the thermal distribution which existed at the instant strain was applied. It should be recalled at this point that pure uranium exhibits three allotropic modifications between room temperature and the melting point—the alpha, beta, and gamma forms. Thus, under the influence of the temperature gradient established during arc-spot welding, these three allotropes, in addition to the liquid phase, were present and subjected to deformation at the instant of straining.

Referring again to Fig. 8, concentric, circular markings can be clearly seen on the specimen surface. The outer extremities of the fusion zone (the inner circle) can be determined by the ripple marks produced during solidification. Also note that epitaxial growth is evidenced by columnar grains common to the fusion zone and the adjacent solid. In the annular ring between the inner circle (fusion zone) and the next circle, the gamma allotropic modification existed at the instant of straining. In like manner, in the next annulus the beta modification existed at the instant of straining. Beyond the outer ring no transformations occurred and the alpha allotrope existed. These conclusions were verified by an analysis of the temperature distribution using both a thermocouple technique and a temperature-sensitive lacquer method.

The rings are apparent because each allotropic modification reacts to the strain applied according to its in-

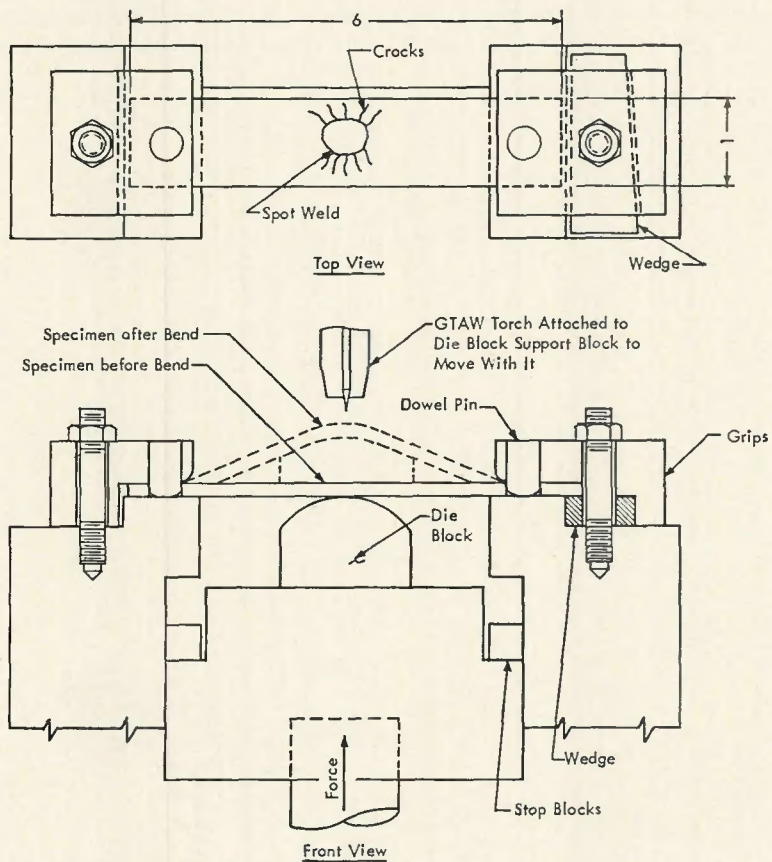

Fig. 5—Spot Varestraint test device showing the way in which a specimen is tested

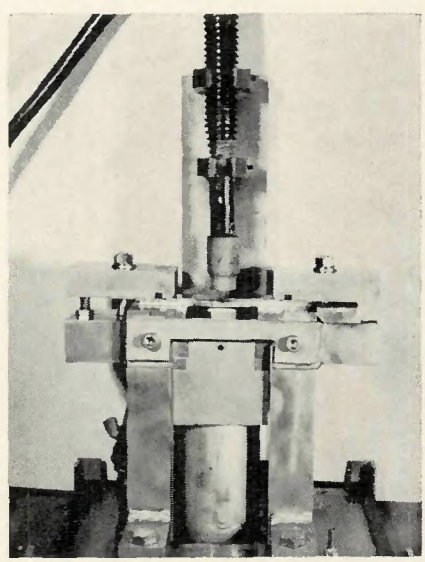

Fig. 6—Front view of the spot Varestraint test device with a specimen in position for testing

herent ductility and modulus of elasticity. The gamma phase is extremely ductile and flows easily under strain. However, the beta phase is brittle and often fractures under the applied strain. In the macrograph of Fig. 8, several beta cracks can be seen, and these will be dealt with in greater detail in Part II at a later date. Thus, the surface relief due to the relative deformability of the alpha, beta, and gamma phases present at the instant of straining, provides built-in markers delineating the extent of the alpha, beta, and gamma zones.

When alloyed uranium is tested, a "new" zone appears outlined on the surface of the tested specimens. This new zone (delineated by crack A-A'-B in Fig. 9) is a result of the gamma-plus-liquid region produced by alloying. This zone is prone to hot cracking and will later be discussed in relation to the cracking mechanism.

It will be noted that the circular markings (Fig. 8) are slightly distorted in elliptical fashion. This configuration is due to the fact that the thermal gradient is also nonsymmetrical. The asymmetrical nature of the thermal gradient results because the specimen width is much narrower than its length. Consequently, the heat-flow pattern is distorted.

Cracks were not found in either the gamma regions or the fusion zone of the unalloyed specimens. Cracks only appeared in these zones when the iron content was increased.

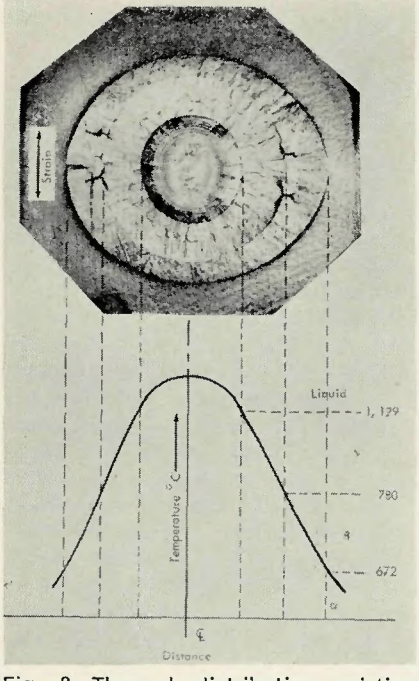

Fig. 8—Thermal distribution existing around an arc-spot weld at the instant of application of augmented strain referred to the as-welded surface characteristics. (Electrolytically etched in a chromic-acetic acid solution)

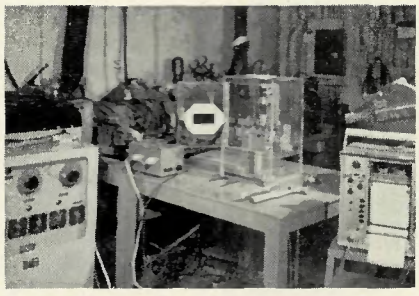

Fig. 7—Tigamajig testing area

Total Crack Length vs. Augmented Strain

The usual method of expressing Varestraint test results is to plot one of the crack measurement criteria, normally the total crack length, versus augmented strain. The various parameters representing chemistry, heat treatment, and the like are held constant for each plot. An example of such a graphical presentation is presented in Fig. 10. The shape of these curves for uranium-iron weld metal is very similar to the shapes of the curves for other alloys that have been tested by the Varestraint method.[7,8] These curves show the relative cracking tendencies for four analyses of weld metal. The most important question, however, relates to the iron content at which cracking begins to occur at a particular strain. This information is shown more clearly by the threshold curve (also referred to as a C curve) in Fig. 11.

Threshold Curve for Cracking Susceptibility

The C curve shows that cracking was not observed in specimens that were spot welded and allowed to cool in the grips of the test device without being bent. Regardless of the iron content, values for this condition (zero-augmented strain) are buttressed by the fact that there were no visible cracks on any of the bead-on-plate electron-beam welds used in preparing the various plates. Weld metal having less than 600 ppm iron was not susceptible to hot cracking at all levels of augmented strains used in testing. For augmented strains less than $^1/_2$%, iron up to 900 ppm did not cause hot cracking. At $^3/_8$% augmented strain, iron contents of 900 to 5,000 ppm caused hot cracking.

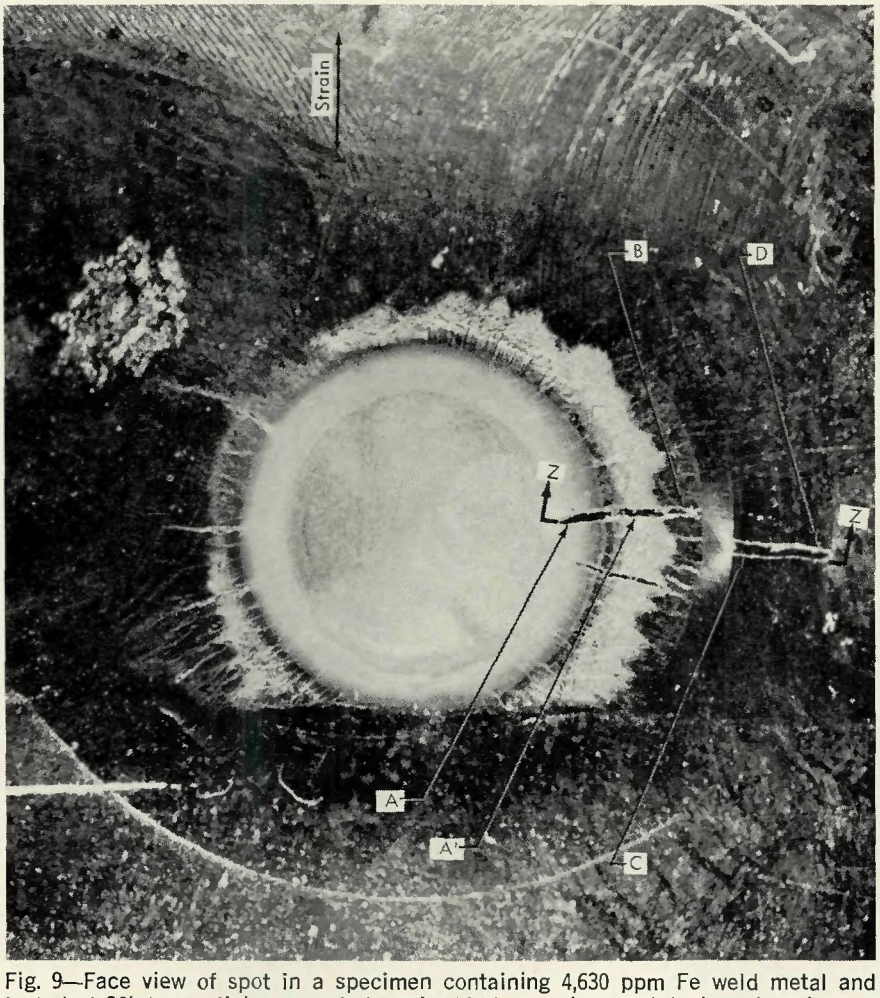

Fig. 9—Face view of spot in a specimen containing 4,630 ppm Fe weld metal and tested at 3% tangential augmented strain. Markers point to alpha-beta interface at D, beta-gamma interface at C, and the liquid-liquid plus gamma boundary at A'. Note that cracks are interrupted by the unliquated gamma zone

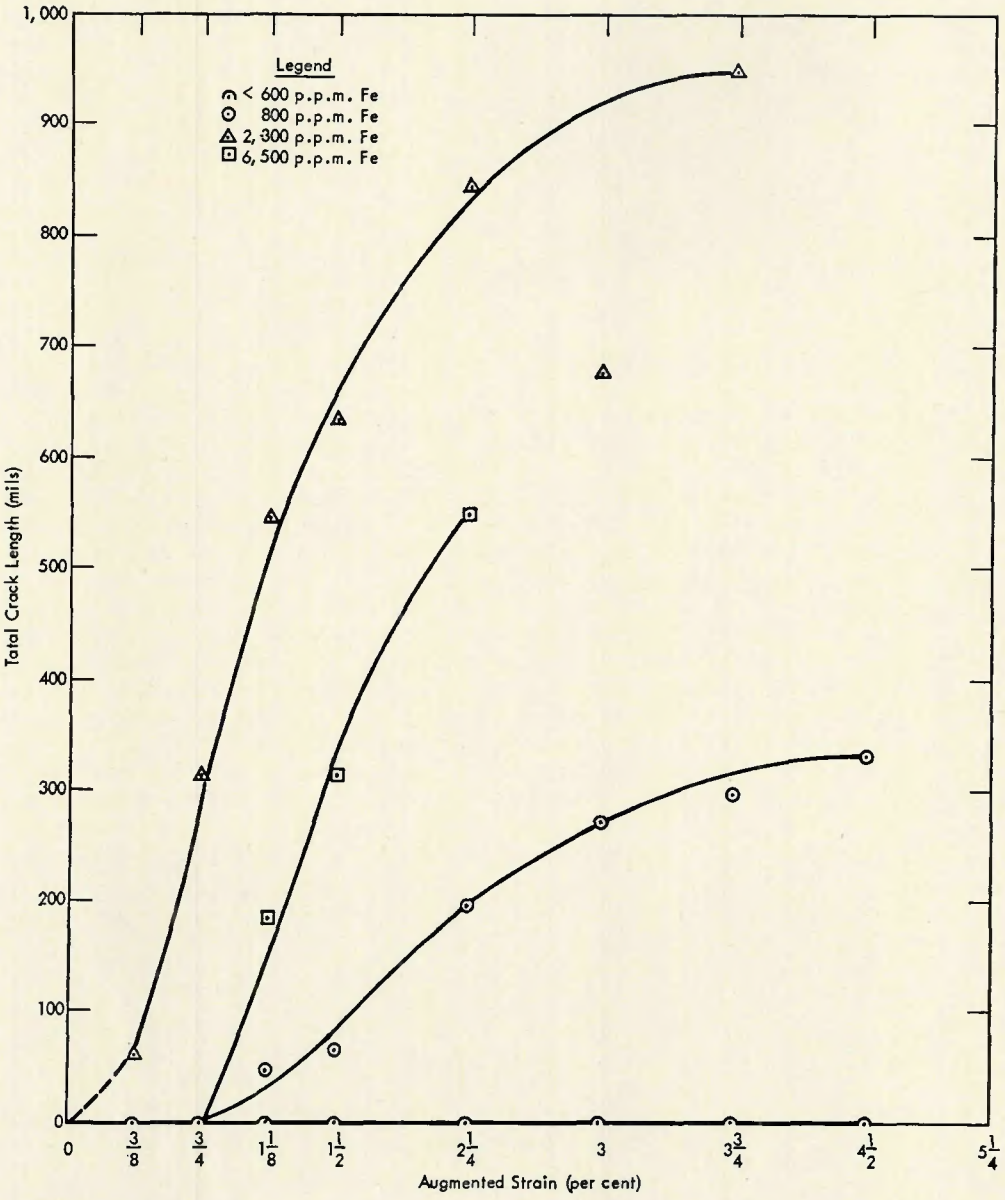

Fig. 10—Total crack length vs. augmented strain for uranium-iron weld metal

ing in many specimens. Thus, $^3/_8$% augmented strain would be considered the threshold augmented strain for hot cracking in this composition range. At high iron concentrations, the hot-cracking tendency vanished at low augmented strains. This behavior has been reported by others for eutectic-type alloys.[9-13]

Cracking in the beta region can occur in low-iron alloys, but the augmented strain required to cause this type of cracking is much higher than strains occurring in the beta phase during welding. Moreover, the tendency for cracking in the beta zone appeared to be independent of iron compositions within the range studied.

Cracking Tendency on a Butt Joint

The joint geometry shown in Fig. 12 was utilized for evaluating the cracking propensity of uranium weld metal alloyed with iron. Iron foil was preplaced in the weld groove in amounts that would provide three zones having different levels of iron. The foil was resistance-spot welded to the face of the joint prior to butting the two plates.

The assembly was tacked by electron-beam welding, then two small beads were welded in opposite directions to partially fuse the iron foil with the base metal. The joint was rewelded by making a gas tungsten-arc pass followed by an electron-beam pass. Then the joint was broken apart, cleaned again, realigned, and arc welded a second time. The next and final pass was made over the arc-welded pass by electron-beam welding. Penetration was nominally 0.1 in. for both processes, and widths of beads were about $^3/_{16}$ and $^3/_8$ in. for the electron-beam process and the gas tungsten-arc process, respectively. Process parameters are listed in Table 4.

After the last pass was made, samples were drilled from the three alloyed zones and analyzed for iron and uranium. Also, cracks were sectioned and analyzed metallographically.

The three iron levels generated by doping the butt joints were chemically analyzed and found to be 6,785, 2,158, and 1,137 ppm iron. These values were very close to the target analyses that were chosen to provide weld metal of both high and low cracking tendencies, as determined by the Tigamajig test results. According to the C curve in Fig. 11, the intermediate iron concentration (2,158 ppm) should be most susceptible to hot cracking, whereas the high-iron (6,785 ppm) alloy should not be hot-crack sensitive unless the strains induced during welding are relatively high. Iron-lean metal (1,137 ppm) should be the least prone to hot cracking.

After gas tungsten-arc welding of the prepared joint, no cracking was visible in any of the iron-alloyed regions; however, it will be shown, sub-

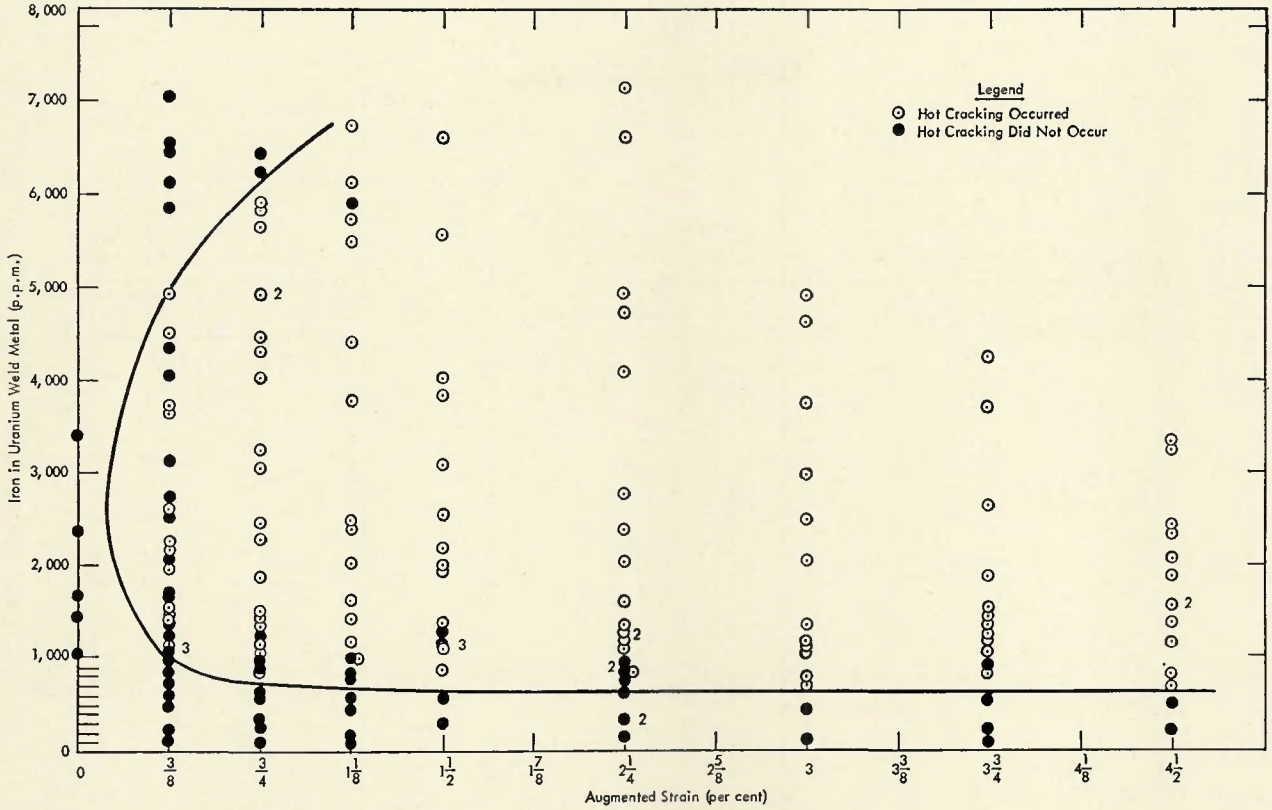

Fig. 11—Threshold curve for the cracking susceptibility of uranium-iron weld metal

sequently, that root cracking did occur in some areas. When the electron-beam pass was made over the previously arc-welded joint, cracking developed in the section having 2,158 ppm iron. Cracking also developed in the transition zone between the high and medium-alloyed sections. The locations of interest are identified in the plan view of this weld in Fig. 13.

A metallographic specimen was cut from each alloyed section. The locations of the sections are indicated in the plan view. Photomicrographs produced from these metallographic specimens illustrate the root cracking tendencies of the welds with different alloy concentrations. The micrograph in Fig. 14 shows the relationship of the cracks in the 1,137 ppm iron weld with respect to the arc-weld fusion zone and the electron-beam-weld fusion zone defined in the macrograph. The slight amount of tearing which occurred in the arc and electron-beam welds is often present in partially penetrated joints of this type, even in pure uranium because of the built-in stress riser at the root.

The severe crack shown in the 2,158 ppm iron weld section of Fig. 15 propagated all the way to the surface, passing through both the arc-weld pass and the electron-beam-weld pass. Apparently, a root crack was initiated in the arc weld, and then it propagated through the electron-beam weld during its solidification and terminated at the surface.

The severity of cracking in the test section containing 6,785 ppm iron was intermediate with respect to that exhibited by the 2,158 and 1,137 ppm iron sections. A macrograph of a short crack at the root of the 6,785 ppm iron section is shown in Fig. 16. The crack in the electron-beam weld apparently propagated from a crack at the root of the previous arc-welded pass.

The results of the actual welding

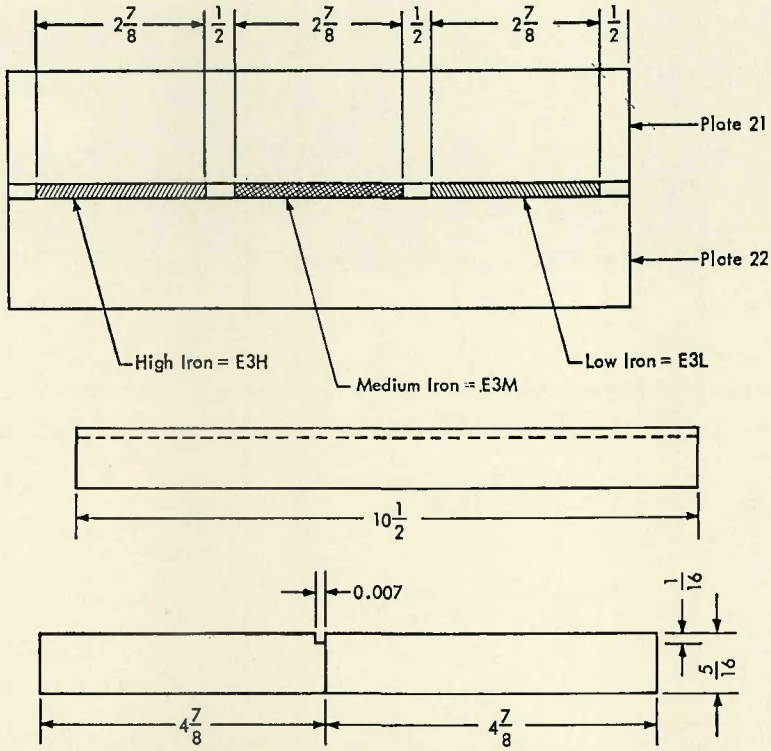

Fig. 12—Joint geometry and placement of the alloying addition for testing the cracking tendency of a partial-penetration weld. Note: Iron alloy additions are inserted at three sections of the weld groove to provide three levels of iron in the weld metal

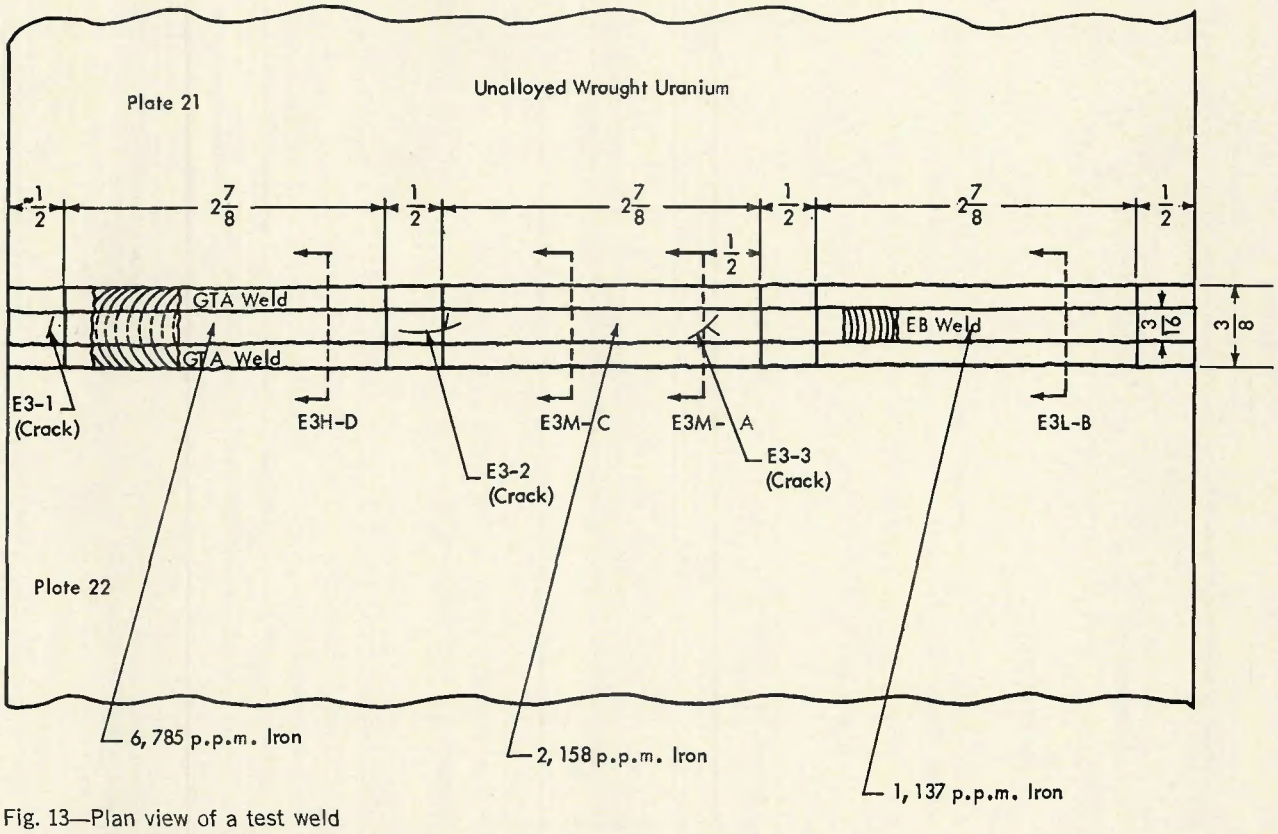

Fig. 13—Plan view of a test weld

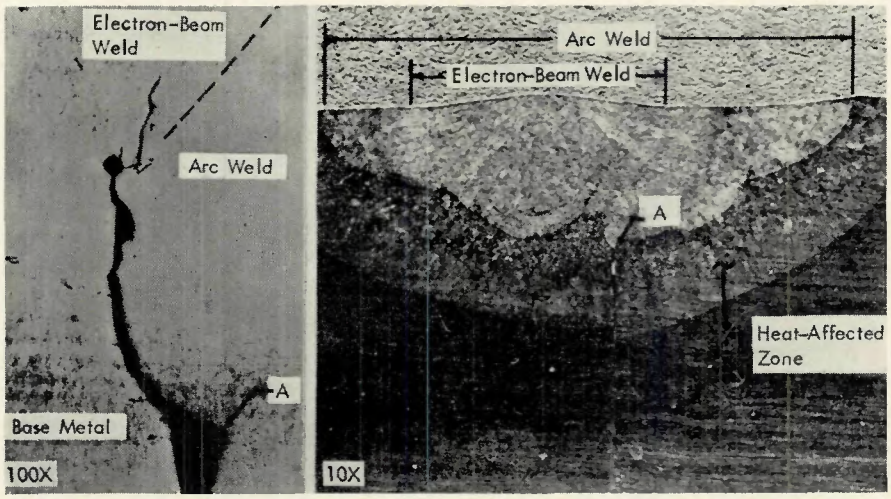

Fig. 14—Welds containing 1,137 ppm iron (reduced 55% on reproduction)

Table 4—Process Parameters for Welding a Uranium-Iron Butt Joint

	Electron beam	Gas tungsten-arc
Current, amp	0.020	200[a]
Voltage, v	110,000	15
Travel Speed, ipm	30	20
Shielding	10^{-4} torr	helium[b]
Electrode	0.012 in. diameter tungsten filament	2% thoriated tungsten, $^1/_8$ in. diameter ground to a point
Distance from heat shield to surface plate, in.	6	—
Filament current, amp	1.9	—
Type of electron gun[c]	R-40	—

[a] Direct current, straight polarity.
[b] A flow rate of 50 cfh was used through a torch equipped with a $^5/_8$ in. diameter metallic shielding cup. Also, 50 cfh was maintained through porous bronze side shields.
[c] The R-40 bias cup is a standard accessory for the separately biased triode gun manufactured by Hamilton Standard, Inc, Windsor Locks, Connecticut.

tests correlate extremely well with the Tigamajig test results. The intermediate iron composition was more prone to hot cracking than either the high- or-low-iron weld metal. Weld metal of intermediate composition must solidify through a relatively wide solidification temperature range. It is characterized by a columnar structure that is unable to accommodate appreciable extension strains at the time that the disappearing liquid phase is film-like and almost continuous. Conversely, the high and low-iron compositions solidify through narrow temperature ranges. In addition, the solid phase is developed sufficiently to withstand or to distribute shrinkage strains. As a consequence, large local strains cannot develop and cause fissuring at sites that are isolated from the mother liquid.

It is noteworthy that the electron-beam weld in the intermediate-iron alloy exhibited a greater hot-cracking tendency than did the gas tungsten-arc weld. The cracking behavior of the welds made by each process is in accord with the hot-cracking model to be described in a future paper.

Conclusions

1. Uranium weld metal having less than 600 ppm (0.06 wt-%) iron is insensitive to hot cracking at augmented strains up to $4^1/_2$%.

2. Welds on butt joints in uranium having up to 900 ppm (0.09 wt-%) iron should not be subject to hot

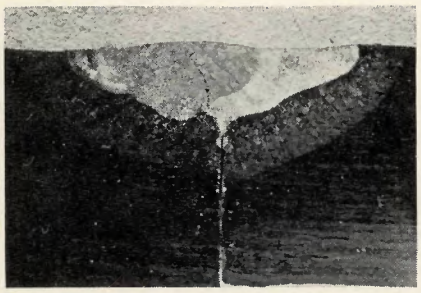

Fig. 15—Cross section of a weld containing 2,158 ppm iron

cracking provided joints are designed to eliminate high restraint.

3. Uranium weld metal with iron contents exceeding 6,000 ppm (0.6 wt-%) are not prone to hot cracking at moderate strain levels.

4. Weld metal intermediate in iron content is very susceptible to hot cracking. The intermediate range is defined by the threshold curve in Fig. 11.

5. Actual welds on uranium butt joints exhibited cracking tendencies similar to that of Varestraint test specimens.

6. The spot-Varestraint test proved to be a useful means of quickly evaluating the thermomechanical effects in the heat-affected zones. The alpha, beta, and gamma phases of uranium were revealed by surface markings characterizing the properties of these phases.

References

1. Gittus, J. H., *Uranium* 220-224 and 447-449, Washington, D. C., Butterworth, Inc. (1963).
2. Rough, F. A., and Bauer, A. A., *Constitution Diagrams of Uranium and Thorium Alloys*, 31-32, Addison-Wesley Publishing Company, Inc. (1959).
3. Elliott, R. P., *Constitution of Binary Alloys*, First Supplement, 440, New York, McGraw-Hill Book Company, Inc. (1965).
4. Swindells, N., "The Solubility of Iron in Solid Uranium Between 0.003 Weight Percent and 0.3 Weight Percent Iron," *Journal of Nuclear Materials*, 18, 261-271 (1966).
5. Turner, P. W., *Effect of Iron on Fissuring of Uranium Weld Metal*, AEC Research and Development Report, Y-1678; Union Carbide Corporation-Nuclear Division, Oak Ridge Y-12 Plant, Oak Ridge, Tennessee; August 11, 1969.
6. Goodwin, G. M., *The Effect of Minor Elements on the Hot Cracking of Inconel 600*, Ph.D. Thesis, Rensselaer Polytechnic Institute, June 1968.
7. Savage, W. F., and Lundin, C. D., "Application of the Varestraint Test to the Study of Weldability," Welding Journal, 45 (11), Research Suppl., 497-s to 503-s (1966).
8. Lee, J. W., Nichols, E. E., and Goodman, S., "Varestraint Testing of Cast 70 Cu-30 Ni Alloy," *Ibid.*, 47 (8), Research Suppl., 371-s to 377-s (1968).
9. Medovar, B. I., "On the Nature of Weld Hot Cracking," *Avtomaticheskaya Svarka*, 7, Four, 12-18 (1954); (Brutcher Translation 3400, Altadena, California).
10. Veroe, J., "The Hot Shortness of Aluminum Alloys," *Metal Industry* (London), 48, 321-491 (1936).
11. Bochvar, A. A., and Sviderskaya, Z. A., "Failure of Castings Caused by Shrinkage Stresses During Crystallization as Related to Composition," Izvestiya An SSSR, Otn., No. 3, 349-354 (1947); (Brutcher Translation 4806, Altadena, California).
12. Hull, F. C., "Effect of Delta Ferrite on the Hot Cracking of Stainless Steel," Welding Journal, 46 (9), Research Suppl., 399-s to 409-s (1967).
13. Medovar, B. I., "Effect of Solubility of Alloying Elements Upon Weld Hot Cracking," *Avtomaticheskaya Svarka*, 8 (2), 79-90 (1955). (Brutcher Translation 3554, Altadena, California).

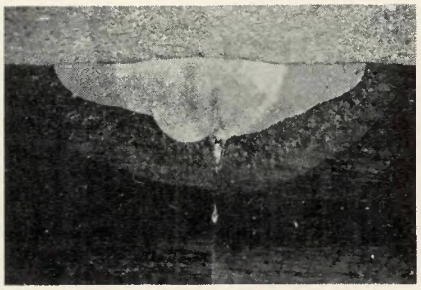

Fig. 16—Cross section of a weld containing 6,785 ppm iron

USSR Welding Research News

By Rudolph O. Seitz

Avtomaticheskaya Svarka 22, No. 4 (April 1970)

• Bel'chuk, G. A. et al.: On the selection of weld sizes in the development of new standards.—The geometric shape and the dimensions of the weld bead were studied. It is shown that a modification of the standards on the size and permissible deviations of the welds is advisable. (47-50).

• Khudonogov, V. N. et al.: A system of recording the operating parameters in friction welding.—A system of recording the operating parameters of friction welding applicable to type Ts MST-75 machines and the principle of operation of this system are described (51-52).

• Subbotovskii, V. P.: Durability of hardfaced Pilger mill rolls.—After a brief outline of existing methods of increasing the wear resistance of Pilger mill rolls by hardfacing a newly developed mechanized process of submerged arc hardfacing is described. Data on the cost of labor for preparing, hardfacing and finishing the rolls and of their durability in service are given (53-56).

• Chvertko, A. I. and Timchenko, V. A.: Equipment with programmed controls for the automation of welding operations.—A brief description is given of source experimental equipment with digital and kinematic program controls of the moving operating organs which has been developed at the E.O. Paton Institute of Electric Welding (57-61).

• Glebov, L. V. and Gorlov, Yu, I.: Heat calculation of welding transformers potted with epoxide compound.—The problems associated with the heat calculation of epoxide potted transformers for resistance welders are discussed. A method of heat calculation with the use of a reduced coefficient of thermal conductivity of the combined insulation between the primary and secondary winding is described (62-64).

• Cherednichok, V. T. et al.: Machine for resistance welding of the foundation members of prefabricated ferroconcrete.—The design of the K-333 machine for the flash butt welding of the T-joints of foundation members of ferroconcrete structures and the welding procedure which has been developed are described (65-69).

Avtomaticheskaya Svarka 23, No. 6 (June 1970)

• Paton, B. E. et al.: Automation of experimental investigations of welding processes (1-6).—The authors describe a system for the automatic collection and processing of experimental data whose application to the study of resistance spot welding has resulted in greater effectiveness of the investigation.

• Okada, K.: The effect of alloying elements on crack formation in the welding of a heat-resistant nickel-base alloy (7-13).—The formation of cracks during the welding of Inconel 713C has been studied. It was found that the cracking resistance is improved by reducing the aluminum content of the alloy.

• Forostovets, B. A. and Kirdo, I. V.: The effect of high-temperature deformation of steel on the presence of a liquid phase on the structure and the properties of welded joints (14-17).—An experimental study has been made

(*Continued on page* 596-s)

RUDOLPH O. SEITZ is Information Specialist with Air Reduction Co., Murray Hill, N. J.